Single-Molecule Magnet Behavior of a Tetranuclear Iron(III) Complex. The Origin of Slow Magnetic Relaxation in Iron(III) Clusters

A. L. Barra,[§] A. Caneschi,[†] A. Cornia,[‡] F. Fabrizi de Biani,[†] D. Gatteschi,*[,†] C. Sangregorio,[†] R. Sessoli,[†] and L. Sorace[†]

Contribution from the Department of Chemistry, University of Florence, Via Maragliano 77, I-50144 Firenze, Italy, Department of Chemistry, University of Modena, Via G. Campi 183, I-41100 Modena, Italy, and High Magnetic Field Laboratory, MPI-CNRS, B.P. 166, 38042 Grenoble, France

Received May 29, 1998. Revised Manuscript Received March 16, 1999

Abstract: The synthesis, crystal structure, and magnetic characterization of a novel tetranuclear iron(III) methoxo-bridged cluster of formula $Fe_4(OCH_3)_6(dpm)_6$ (where Hdpm = dipivaloylmethane) is reported. The cluster has a ground spin state of $S = 5$, which is selectively populated below 20 K. High-field EPR spectra revealed that the system has a uniaxial magnetic anisotropy, corresponding to a zero field splitting parameter $D = -0.2$ cm^{-1} of the $S = 5$. Such anisotropy below 1 K gives rise to the slow relaxation of the magnetization similar to that of super-paramagnets. To investigate the origin of the magnetic anisotropy we have evaluated the projection of the single-ion and dipolar contributions to the zfs of the ground state. The zfs tensors of the three structurally independent iron(III) centers have been calculated from the coordination geometry and spectroscopic data using the angular overlap model. To test the reliability of the approach high-field EPR spectra of the parent monomer $Fe(dpm)_3$ have been recorded to compare the calculated and experimental zfs parameters.

Introduction

Molecular clusters of magnetic transition metal ions have been attracting increasing interest since the discovery that they can behave as nanomagnets and show magnetic bistability of pure molecular origin.[1,2] The first cluster which was proved to have relaxation of the magnetization as slow as 2 months at low temperature is $[Mn_{12}O_{12}(CH_3COO)_{16}(H_2O)_4]$ (Mn12Ac),[3,4] which has a magnetic hysteresis cycle below 4 K similar to that observed for bulk magnets.[5] For this reason it was claimed to be an example of single-molecule magnet. The magnetic bistability associated with the hysteresis cycle in principle can be used for information storage. The important feature of this compound is that the hysteresis has a molecular origin, as confirmed by the observation of magnetic hysteresis in frozen solutions[6] and in polymer films,[7] which rule out any possibility of cooperative magnetic behavior.

Another unique feature of Mn12Ac at low temperature is that quantum effects seem to dominate the reversal of the magnetization, giving a peculiar steplike magnetic hysteresis cycle.[8] The system is thus multistable and particularly appealing for potential technological applications aiming to the so-called quantum computers.

The slow relaxation of the magnetization, which is at the origin of the interesting behavior, is due to the presence of an energy barrier to be overcome in the reversal of the magnetic moment. At the simplest level of approximation the relaxation time follows a thermally activated behavior:[9]

$$\tau = \tau_0 \exp(\Delta/k_B T) \qquad (1)$$

where Δ is the height of the barrier and τ_0 is the pre-exponential factor.

The height of the barrier is related to the spin of the ground state and to the magnetic anisotropy. Slow relaxation of the magnetization was observed by Mössbauer spectroscopy in some iron clusters,[10] and this behavior, which is analogous to that observed in super-paramagnetic particles, was attributed to shape anisotropy effects.[11] However it is now established that in molecular clusters the anisotropy is magnetocrystalline in nature, i.e. it is associated with the zero field splitting of the ground

[†] University of Florence.
[‡] University of Modena.
[§] H. M. F. L., Grenoble.

(1) (a) Gatteschi, D.; Caneschi, A.; Pardi, L.; Sessoli, R. *Science* **1994**, *265*, 1054. (b) Awschalom, D. D.; Di Vincenzo, D. P. *Phys. Today* **1995**, 43.

(2) a) Aubin, S. M. J.; Wemple, M. W.; Adams, D. M.; Tsai, H.-L.; Christou, G.; Hendrickson, D. N. *J. Am. Chem. Soc.* **1996**, *118*, 7746. (b) Aubin, S. M. J.; Dilley, N. R.; Wemple, M. W.; Maple, M. B.; Christou, G.; Hendrickson, D. N. *J. Am. Chem. Soc.* **1998**, *120*, 839. (c) Mallah, T.; Auberger, C.; Verdaguer, M.; Veillet, P. *J. Chem. Soc., Chem. Commun.* **1995**, 61. (d) Vernier, N.; Bellessa, G.; Mallah, T.; Verdaguer, M. *Phys. Rev. B* **1997**, *56*, 75.

(3) Lis, T. *Acta Crystallogr., Sect. B* **1980**, *36*, 2042.

(4) Caneschi, A.; Gatteschi, D.; Sessoli, R.; Barra, A.-L.; Brunel, L.-C.; Guillot, M. *J. Am. Chem. Soc.* **1991**, *113*, 5873.

(5) Sessoli, R.; Gatteschi, D.; Caneschi, A.; Novak, M. A. *Nature* **1993**, *365*, 141.

(6) Cheesman, M. R.; Oganesyan, V. S.; Sessoli, R.; Gatteschi, D., Thomson, A. *J. Chem. Commun.* **1997**, 1677.

(7) Eppley, H. J.; Tsai, H.-L.; de Vries, N.; Folting, K.; Christou, G.; Hendrickson, D. N. *J. Am. Chem. Soc.* **1995**, *117*, 301.

(8) a) Friedman, J.; Sarachick, M. P.; Tejada, J.; Maciejewski, J.; Ziolo, R. *Phys. Rev. Lett.* **1996**, *76*, 3820. (b) Thomas, L.; Lionti, F.; Ballou, R.; Gatteschi, D.; Sessoli, R.; Barbara, B. *Nature* **1996**, *383*, 145.

(9) Morrish, A., H. *The Physical Principles of Magnetism*; Wiley & Sons: Inc. New York, 1966; p 360.

(10) Taft, K. L.; Papaefthymiou, G. C.; Lippard, S. J. *Science* **1993**, *259*, 1302.

(11) Papaefthymiou, G. C. *Phys. Rev. B* **1992**, *46*, 366.

10.1021/ja9818755 CCC: $18.00
Published on Web 05/20/1999

state. To have a barrier the system must have an Ising-type anisotropy, which corresponds to a negative zero field splitting, i.e. to have the $M = \pm S$ states lying lowest. In the case of axial symmetry, for a system with integer spin in the ground state, the energy barrier can be associated with the energy difference between the lowest $M = \pm S$ states and the highest $M = 0$ state, with a negative D parameter, which is defined by the usual spin Hamiltonian, $H = DS_z^2$.

$$\Delta = |D|S^2 \tag{2}$$

At low temperature the clusters will be either in the $M = -S$ or in the $M = +S$ ground levels. The inversion of the magnetization corresponds to the relaxation from say $-S$ to $+S$. To do this the system climbs up all the ladder of levels, one step at a time from $M = -S$ to $M = -S + 1$ up to $M = 0$, and then descends down.[12] Although this is clearly an approximation it has been shown to hold reasonably well for other molecular magnetic clusters.[5]

It has been suggested that the relaxation time for this thermally activated process is given by

$$t \propto (S^6/\Delta^3) \exp(\Delta/k_B T) \tag{3}$$

To design and synthesize new nanomagnetic materials based on molecular clusters it is therefore necessary to achieve a large S ground spin state. This can be done even using a small number of ions if the individual components have a large spin. For this purpose ions such as high-spin manganese(II), manganese(III), iron(III) appear to be well-suited. The second requirement to be met in order to have slow relaxation is the control of the magnetic anisotropy. To choose the appropriate building blocks, it is necessary to know under which conditions large and negative zero field splitting can be observed and to rationalize how the zero field splitting of the cluster is related to those of the single ions. In principle, one can expect that the zero field splitting of clusters is determined by single ion anisotropy and by spin−spin interactions which can be both magnetic dipolar and exchange in nature.

High-spin iron(III), which has $S = {}^5/_2$, is a promising building block to achieve large S in the ground state. A drawback of this ion is its ^{6}S nature, which in principle does not give rise to large anisotropies. However the zero field splitting for pseudo-octahedral iron(III) complexes coordinated to oxygen atoms has been determined by EPR spectroscopy and found to reach up to 0.3 cm^{-1},[13] but its sign cannot be easily established in a conventional experiment. A confirmation to this possibility of using iron(III) for single-molecule magnets comes from an octanuclear iron(III) cluster, which has a ground $S = 10$ state, and $D = -0.19$ cm^{-1}, which shows slow magnetic relaxation in the Mössbauer spectra at ca. 30 K and magnetic hysteresis below 1 K.[14] Due to the complexity of the system it was however impossible to quantitatively justify the observed zero field splitting, i.e. attributing it to single ion contributions, to spin−spin contributions, or to both.

We present here the synthesis, structure, and the magnetic characterization of a tetranuclear iron(III) cluster of formula $Fe_4(OCH_3)_6(dpm)_6$ (**1**) (where Hdpm = dipivaloylmethane), which has a $S = 5$ ground state and shows superparamagnetic-like behavior. The zero field splitting of the ground state has been precisely determined through high-field, high-frequency EPR (HF-EPR) spectra and compared to the expected value obtained by an estimation of the crystal field effects performed by using the angular overlap model (AOM). To test this approach HF-EPR spectra of $Fe(dpm)_3$ were recorded.

We suggest that this compound as a case history that can shed light on the origin of magnetic anisotropy of iron(III) clusters and more generally indicate which criteria must be met to achieve single-molecule magnets.

Table 1. Crystal Data and Structure Refinement for $[Fe_4(OCH_3)_6(dpm)_6]$ (**1**)

formula	$Fe_4C_{72}H_{132}O_{18}$
fw	1509.18
crystal system	monoclinic
space group[a]	*C*2/*c* (no. 15)
color of crystal	yellow
a, Å	29.217(5)
b, Å	15.996(5)
c, Å	18.244(5)
α, deg	
β, deg	94.965(10)
γ, deg	
V, Å^3	8494(4)
Z	4
*R*1, w*R*2 [b]	0.0750, 0.2509
GOF[c]	1.084

[a] Hahn, T., Ed. *International Tables for X-ray Crystallography*; D. Reidel: Dordrecht, The Netherlands, 1983. [b] $R1 = \sum||F_o| - |F_c||/\sum|F_o|$; $wR2 = (\sum[w(F_o^2 - F_c^2)^2]/\sum[wF_o^4])^{1/2}$. [c] GOF $= [\sum[w(F_o^2 - F_c^2)^2]/(n - p)]^{1/2}$, where n is the number of reflections used for refinement, p is the total number of parameters refined, and $w = 1/[\sigma^2(F_o^2) + (0.1528P)^2 + 0.0000P]$ with $P = (\mathrm{Max}(F_o^2,0) + 2F_c^2))/3$.

Experimental Section

Synthetic Procedures. All operations were carried out under the exclusion of moisture, unless otherwise stated. $NaOCH_3$ was purchased from Fluka as a ~5.4 M solution in methanol. $LiOCH_3$, $FeCl_2$, $FeCl_3$, and Hdpm were obtained from Aldrich and used as received. Methanol (Fluka) was distilled over $Mg(OCH_3)_2$ shortly before use.

(a) To a solution of 0.859 g (6.8 mmol) of $FeCl_2$ in 25 mL of anhydrous methanol were added slowly 1.25 g (6.8 mmol) of Hdpm and later 0.62 g (13.6 mmol) of $LiOCH_3$ under argon. The resulting red solid was filtered under argon flux, washed with anhydrous methanol, and exposed to the air. A 0.1 g sample of the yellow solid obtained was dissolved in Et_2O:methanol (2:1 v/v, 60 mL). Yellow rodlike crystals of **1** were obtained by slow evaporation of the solvent with ca. 20% yield.

(b) To a solution of 0.406 g (2.5 mmol) of $FeCl_3$ in 20 mL of anhydrous methanol was added 0.461 g (2.5 mmol) of Hdpm with vigorous stirring, resulting in a deep red solution. Subsequent addition of 5.9 mmol of $NaOCH_3$ (1.1 mL) led to a orange-yellow precipitate, which was isolated by filtration (G4), washed with anhydrous methanol, and dried under vacuum. Crystals of **1** were reproducibly obtained by dissolving the yellow solid (0.25 g) in Et_2O:methanol (2:1 v/v, 30 mL) and by either slow evaporation of the solvent or slow diffusion of methanol vapors in a sealed vessel (yield 45%). Anal. Calcd for **1**, $C_{72}H_{132}Fe_4O_{18}$: C, 57.30; H, 8.82. Found: C, 56.98; H, 8.93.

X-ray Structure Determination. Compound **1** crystallizes in the form of air-stable yellow rods. A well-shaped 0.12 × 0.14 × 0.20 mm individual was chosen for X-ray data collection, which was performed at 200(2) K on an Enraf-Nonius CAD-4 four-circle diffractometer equipped with graphite-monochromated Cu Kα radiation and a low-temperature facility. Accurate unit cell parameters and other experimental details are reported in Table 1. Intensity data were collected and corrected for absorption (empirical) and *Lp* effects. The symmetry and systematic absences of the reciprocal lattice were found to be consistent with the monoclinic space groups *Cc* (no. 9) and *C*2/*c* (no.

(12) Villain, J.; Hartman-Boutron, F.; Sessoli, R.; Rettori, A. *Europhys. Lett.* **1994**, *27*, 159.

(13) Bencini, A.; Gatteschi, D. In *Transition Metal Chemistry;* Nelson, G. A., Figgis, B. M., Eds; Dekker: New York, 1982; Vol. 8.

(14) (a) Wieghardt, K.; Phol, K.; Jibtil, I.; Huttner, G. *Angew. Chem., Int. Ed. Engl.* **1984**, *23*, 77. (b) Barra, A.-L.; Debrunner, P.; Gatteschi, D.; Schulz, C. E.; Sessoli, R. *Europhys Lett.* **1996**, *35*, 133.

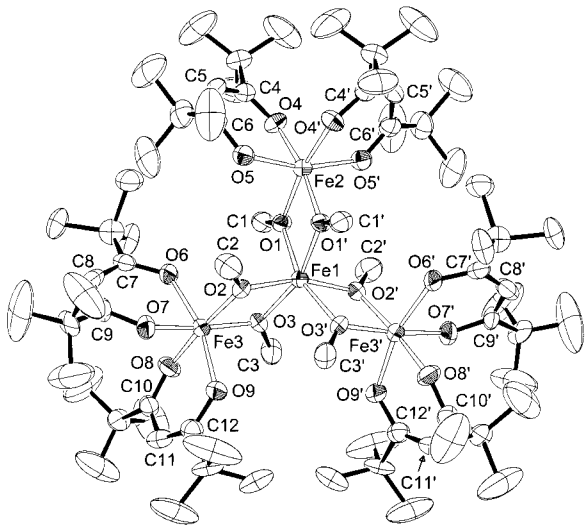

Figure 1. ORTEP drawing showing the molecular structure of **1** with displacement ellipsoids at 30% probability level and the atom labeling scheme. Primed atoms are related to unprimed ones by a crystallographic 2-fold axis passing through Fe1 and Fe2. Only the 0.70-occupancy arrangement of dpm ligands around Fe3 is shown. Hydrogen atoms have been omitted and *t*-Bu groups not labeled for clarity.

15). The structure was solved in both space groups by direct methods,[15] which gave the positions of all non-hydrogen atoms but few carbon atoms of the *t*-Bu groups. Atom coordinates were found to be fully consistent with the centrosymmetric space group *C*2/*c*, which was assumed in subsequent refinement cycles on F^2 by full-matrix least-squares techniques using SHELX93.[16] Disorder effects in the coordination environment of Fe3, arising from different arrangements of dpm ligands, were individuated in ΔF maps and successfully modeled by assigning 0.70 occupancy to dpm ligands binding through O6−O7 and O8−O9 (see Figure 1) and 0.30 occupancy to dpm ligands binding through O6−O8 and O7−O9 (not shown). The geometry of latter dpm anions was restrained to that of the nondisordered ligands around Fe2 (although the torsion angles of *t*-Bu groups were refined). The two 0.30-occupancy dpm ligands were refined isotropically, while anisotropic displacement parameters were used for all the remaining non-hydrogen atoms in the structure. Since disorder of dpm oxygens could not be resolved, full site occupancies were assigned to O4, O5, O6, O7, O8, and O9, which showed normal displacement ellipsoids. Hydrogen atoms were added at calculated positions assuming an idealized bond geometry and C−H distances of 0.98 and 0.95 Å for methyl and methine hydrogens, respectively. The torsion angles of methoxide CH_3 groups were estimated from circular difference Fourier syntheses and then held fixed. Several cycles of refinement led to reasonable convergence with $R1 = 0.075$ and w$R2 = 0.2509$. The major disorder effects described above, together with the large displacement parameters of the *t*-Bu carbon atoms, may account for the very weak diffracting power of the crystals and for the relatively high *R* factors. The data collection have been performed also with the Mo Kα radiation, but no improvement in the determination of the structure has been achieved. Selected bond distances and angles are provided in Table 2, while other crystallographic data are given as Supporting Information.

Magnetic Measurements and EPR Spectra. The temperature dependence of the static magnetic susceptibility has been measured with a Metronique MS02 SQUID magnetometer at 1.0 T and 10 mT. The data were corrected for the contribution of the sample holder and for the diamagnetism of the sample estimated from Pascal's constants. The ac magnetic susceptibility has been measured with a home-built ac susceptometer equipped with a ^{3}He/^{4}He dilution refrigerator by the Centre des Recherches sur les Tres Basses Temperatures in Grenoble (France).

Polycrystalline powder EPR spectra were recorded at X-band frequency on a Varian ESR9 spectrometer equipped with a continuous-flow ^{4}He cryostat. High-field EPR spectra were recorded on a laboratory-made spectrometer[17] using powder samples pressed in pellets to avoid preferential orientation of the crystallites in the strong magnetic field. Two types of radiation source have been used: an optically pumped far-infrared laser (245 GHz) and a Gunn diode operating at 95 GHz and equipped with a second- and third-harmonic generator to record spectra at 190 and 285 GHz. [17]

Table 2. Selected Interatomic Distances (Å) and Angles (deg) for $[Fe_4(OCH_3)_6(dpm)_6]$ (**1**)[a]

Fe(1)···Fe(2)	3.146(2)	Fe(1)···Fe(3)	3.133(1)
Fe(2)···Fe(3)	5.372(2)	Fe(3)···Fe(3′)	5.550(2)
Fe(1)−O(1)	2.010(4)	Fe(1)−O(2)	2.010(5)
Fe(1)−O(3)	2.017(5)	Fe(2)−O(1)	1.975(5)
Fe(2)−O(4)	1.992(5)	Fe(2)−O(5)	2.026(5)
Fe(3)−O(3)	1.950(5)	Fe(3)−O(2)	1.954(5)
Fe(3)−O(8)	1.996(6)	Fe(3)−O(7)	1.999(6)
Fe(3)−O(6)	2.015(5)	Fe(3)−O(9)	2.019(5)
Fe(2)···Fe(1)···Fe(3)	117.65(3)	Fe(3)···Fe(1)···Fe(3′)	124.70(6)
Fe(3)···Fe(2)···Fe(3′)	62.20(3)	Fe(2)···Fe(3)···Fe(3′)	58.90(2)
O(1)−Fe(1)−O(2′)	93.0(2)	O(1)−Fe(1)−O(2)	101.3(2)
O(2′)−Fe(1)−O(2)	162.0(3)	O(1)−Fe(1)−O(1′)	75.0(3)
O(1)−Fe(1)−O(3′)	160.9(2)	O(2)−Fe(1)−O(3)	74.1(2)
O(2)−Fe(1)−O(3′)	94.3(2)	O(1)−Fe(1)−O(3)	93.4(2)
O(3′)−Fe(1)−O(3)	101.5(3)	O(1′)−Fe(2)−O(1)	76.5(3)
O(1)−Fe(2)−O(4′)	169.0(2)	O(1)−Fe(2)−O(4)	93.3(2)
O(4)−Fe(2)−O(4′)	97.1(3)	O(1)−Fe(2)−O(5)	100.1(2)
O(1)−Fe(2)−O(5′)	93.1(2)	O(4)−Fe(2)−O(5′)	84.5(2)
O(4)−Fe(2)−O(5)	84.4(2)	O(5′)−Fe(2)−O(5)	163.2(3)
O(3)−Fe(3)−O(2)	76.9(2)	O(3)−Fe(3)−O(8)	94.3(2)
O(2)−Fe(3)−O(8)	171.2(2)	O(3)−Fe(3)−O(7)	171.5(2)
O(2)−Fe(3)−O(7)	94.6(2)	O(8)−Fe(3)−O(7)	94.2(2)
O(3)−Fe(3)−O(6)	96.0(2)	O(2)−Fe(3)−O(6)	96.2(2)
O(8)−Fe(3)−O(6)	84.3(2)	O(7)−Fe(3)−O(6)	84.5(2)
O(3)−Fe(3)−O(9)	96.4(2)	O(2)−Fe(3)−O(9)	96.3(2)
O(8)−Fe(3)−O(9)	84.8(2)	O(7)−Fe(3)−O(9)	84.7(2)
O(6)−Fe(3)−O(9)	164.1(2)	Fe(2)−O(1)−Fe(1)	104.2(2)
Fe(3)−O(2)−Fe(1)	104.4(2)	Fe(3)−O(3)−Fe(1)	104.3(2)

[a] Primed atoms are related to unprimed ones by a 2-fold axis passing through Fe1 and Fe2.

Results and Discussion

Synthesis. Synthetic approaches based on β-diketonates and alkoxides are of general utility for assembling transition metal clusters.[18] The application of this strategy to iron chemistry was prompted by the observation that iron molecular alkoxides may represent potential candidates for obtaining single-molecule magnets. In the adopted synthetic procedure, β-diketones with apolar substituents are allowed to react with 1 equiv of $FeCl_3$ and an alkali-metal methoxide in methanol, giving insoluble products of approximate composition $[Fe(OCH_3)_2(L)]_n$ that can be recrystallized from organic solvents. In this way, molecular alkoxides with different nuclearity and connectivity have been isolated by simply varying the substituents on the β-diketonate ligands, by varying the combination of solvents employed for

(15) Altomare, A.; Burla, M. C.; Camalli, M.; Cascarano, G.; Giacovazzo, C.; Guagliardi, A.; Polidori, G.; Spagna, R.; Viterbo, D. *J. Appl. Chem.* **1989**, *22*, 389

(16) Sheldrick, G. M. *SHELXL-93, Program for Crystal Structure Refinement*, University of Goettingen, Goettingen (RFG), 1993.

(17) (a) Barra, A.-L.; Brunel, L. C.; Robert, J. B. *Chem. Phys. Lett.* **1990**, *165*, 107. (b) Muller, F.; Hopkins, M. A.; Coron, N.; Grynberg, M.; Brunel, L. C.; Martinez, G. *Rev. Sci. Instrum.* **1989**, *60*, 3681.

(18) (a) Bertrand, J. A.; Ginsberg, A. P.; Kaplan, R. I.; Kirkwood, C. E.; Martin, R. L.; Sherwood, R. C. *Inorg. Chem.* **1971**, *10*, 240. (b) Taft, K. L.; Caneschi, A.; Pence, L. E.; Delfs, C. D.; Papaefthymiou, G. C.; Lippard, S. J. *J. Am. Chem. Soc.* **1993**, *115*, 11753. (c) Pence, L. E.; Caneschi, A.; Lippard, S. J. *Inorg. Chem.* **1996**, *35*, 3069. (d) Abbati, G. L.; Cornia, A.; Fabretti, A. C.; Caneschi, A.; Gatteschi, D. *Inorg. Chem.* **1998**, *37*, 1430. (e) Abbati, G. L.; Cornia, A.; Fabretti, A. C.; Caneschi, A.; Gatteschi, D. *Inorg. Chem.* **1998**, *37*, 3759.

Scheme 1

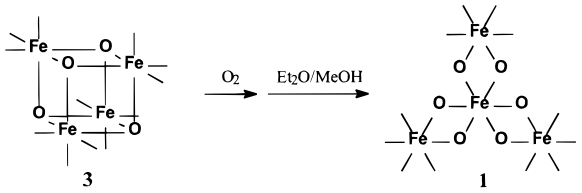

crystallization, or by adding potential templants[18,19] By using Hdpm in this procedure, crystallization from Et_2O:methanol mixtures gives the novel tetrairon(III) cluster **1** in good yield, whereas $CHCl_3$:methanol solutions afford crystals of $[Fe_2(OCH_3)_2(dpm)_4]$ (**2**).[20] In an alternative approach, we first assembled the tetrairon(II) cubane complex $[Fe_4(OCH_3)_4(dpm)_4(HOCH_3)_4]$ (**3**) from iron(II) chloride, 2 equiv of $LiOCH_3$, and 1 equiv of Hdpm in methanol, as reported by Lippard et al.[18b] Compound **3** is extremely air-sensitive in the solid state, and its color readily turns from red to yellow by contact with dioxygen. The oxidation product of Lippard's complex is still unidentified, although it retains a high solubility in moderately polar organic solvents. The hydrophobic shell of bulky *t*-Bu groups is therefore most probably preserved, although major rearrangements of the core cannot be excluded. Crystallization of the air-oxidized material from Et_2O:methanol mixtures reproducibly gives **1** as the major product and possibly small quantities of the dimer **2**, which forms large orange plates.

Although self-assembly reactions are extensively used to synthesize molecular clusters, the design and synthesis of new molecules is seriously hampered by a lack of control on the nuclearity, the connectivity, and more generally the structural parameters of the products. We have already suggested that the common tendency of iron(III) and manganese(III) molecular alkoxides to display layered closest packing (c.p.) cores may represent a starting point for addressing the synthesis of large magnetic clusters.[18d] The layered $[Fe^{III}_4(OCH_3)_6]^{6+}$ core of **1**, obtained either by oxidation and rearrangement of the $[Fe^{II}_4(OCH_3)_4]^{4+}$ precursor (Scheme 1) or directly from $FeCl_3$, illustrates this possibility. Several alkoxoiron(III) complexes containing methoxide and β-diketonate ligands have been synthesized by the same procedure, including Fe_2,[20] Fe_3,[19a] Fe_6,[19b−d] and Fe_{10}[19e] species. Recent investigations have shown that β-diketonate-assisted methanolysis can be used to synthesize manganese molecular alkoxides as well. Starting from manganese(II) salts, low-valent cubane Mn_4 complexes have been obtained under the strict exclusion of air,[18c] whereas a ringlike Mn^{III}_6 cluster[18d] and a mixed valent $Mn^{II}_3Mn^{III}_4$ complex,[18e] both featuring a layered core, have been isolated as products of a partial air oxidation.

Crystal Structure. Figure 1 shows an ORTEP drawing of $[Fe_4(OCH_3)_6(dpm)_6]$. The molecule has 2-fold symmetry due to the presence of a crystallographic C_2 axis passing through Fe1 and Fe2. The four Fe atoms lie exactly on a plane, the inner Fe atom being in the center of an isosceles triangle. The intramolecular Fe···Fe distances are 3.146(2) Å for the Fe1−Fe2 couple and 3.133(1) Å for the Fe1−Fe3 one. The edges take the values of 5.372(2) Å (Fe2···Fe3 and Fe2···Fe3′) and 5.550(2) Å (Fe3···Fe3′), while Fe2···Fe1···Fe3 and Fe3···Fe1···Fe3′ angles are 117.65(3) and 124.70(6)°, respectively. Three bis(μ-OCH_3) ligands connect the central Fe1 atom to the three peripheral ones, which complete their coordination by binding two dipivaloylmethanide anions. The Fe−O−Fe angles at the bridging methoxide ligands are equal within experimental error, taking the value 104.3(2).

All the iron(III) atoms have a highly distorted octahedral environment but different types of distortion. The central iron(III) atom Fe1 binds to methoxide ligands only, and the Fe1−O distances are equal within σ (av 2.012(4) Å). Examination of interbond angles shows that the coordination environment of Fe1 approaches 3-fold symmetry quite closely. The coordination geometry of Fe2 and Fe3 is somewhat more irregular due to the presence of both methoxide and dpm anions. In particular, the peripheral metal ions form shorter bonds with OMe than with dpm ligands. While the average Fe−O(Me) separation is 1.975(5) Å for Fe2 and 1.952(5) Å for Fe3, Fe−O(dpm) distances range from 1.992(5) to 2.026(5) Å. More detailed examination of Table 2 shows that Fe−O(dpm) distances can be grouped in two sets, comprising Fe−O bonds cis and trans to methoxide ligands (av 2.020(6) and 1.996(4) Å, respectively). A similar asymmetric binding mode of dpm was previously observed in the dimer $[Fe_2(OCH_3)_2(dpm)_4]$.[20] The O−Fe−O "bite" angles of dpm ligands are very similar to each other (av 84.6(2)°) and larger than those involving OMe anions. The pattern of bond distances and angles so far described indicates that the peripheral metal ions have quite similar coordination environments, with either crystallographically imposed (for Fe2) or idealized (for Fe3) 2-fold symmetry along the Fe2−Fe1 and Fe3−Fe1 directions, respectively.

The Fe1−O2−Fe3−O3 moiety is nearly planar (maximum deviation 0.03 Å) and forms dihedral angles of 99.5 and 105.9° with the planes through Fe1−O1−Fe2−O1′ and Fe1−O2′−Fe3′−O3′, respectively. Consequently, the molecule has a propeller shape and is chiral. However, the space group is centrosymmetric so the two enantiomeric species are both present in the crystal. An interesting feature of the structure is represented by the so-far-neglected disorder in the coordination environment of Fe3. Detailed examination of difference Fourier electron density maps revealed the presence of 0.30-occupancy dpm ligands in a different spatial arrangement with respect to that shown in Figure 1. This point is best illustrated by referring to the overall structure of the Fe/O core, which comprises two parallel layers of c.p. oxygen atoms (maximum deviation 0.26 Å), one on each side of the Fe_4 moiety. Each dpm anion can provide two oxygen donors on either the same or different oxygen layer, the last type of coordination having the largest probability.

In the crystal, the tetramers are well-isolated from each other and there are no intermolecular contacts between the Fe atoms shorter than 9 Å.

Although the topology of the metal ions in **1** bears direct resemblance with that found in either homo-[21] or heterometallic[22] tetranuclear complexes, the molecular structure is unique among polyiron(III) complexes. The efficiency of OMe ligands in promoting aggregation is well-demonstrated by the presence of

(19) a) Caneschi, A.; Cornia, A.; Fabretti, A. C.; Gatteschi, D.; Malavasi, W. *Inorg. Chem.* **1995**, *34*, 4660. (b) Caneschi, A.; Cornia, A.; Lippard, S. J. *Angew. Chem., Int. Ed. Engl.* **1995**, *34*, 467. (c) Caneschi, A.; Cornia, A.; Fabretti, A. C.; Foner, S.; Gatteschi, D.; Grandi, R.; Schenetti, L. *Chem. Eur. J.* **1996**, *2*, 1379. (d) Abbati, G. L.; Caneschi, A.; Cornia, A.; Fabretti, A. C.; Gatteschi, D.; Malavasi, W.; Schenetti, L. *Inorg. Chem.* **1997**, *36*, 6443. (e) Caneschi, A.; Cornia, A.; Fabretti, A. C.; Gatteschi, D. *Angew. Chem., Int. Ed. Engl.* **1995**, *34*, 2716.

(20) Le Gall, F.; Fabrizi de Biani, F.; Caneschi, A.; Cinelli, P.; Cornia, A.; Fabretti, A. C.; Gatteschi, D. *Inorg. Chim. Acta* **1997**, *262*, 123.

(21) (a) Güdel, H. U.; Hauser, U. *Inorg. Chem.* **1980**, *19*, 1325. (b) Andersen, P.; Damhus, T.; Pedersen, E.; Petersen, A. *Acta Chem. Scand.* **1984**, *A38*, 359. (c) Gordon-Wylie, S. W.; Bominaar, E. L.; Collins, T. J.; Workman, J. M.; Claus, B. L.; Patterson, R. E.; Williams, S. A.; Conklin, B. J.; Yee, G. T.; Weintraub, S. T. *Chem. Eur. J.* **1995**, *1*, 528.

(22) Hodgson, D. J.; Michelsen, k.; Pedersen, E., Towle, D. K. *Inorg. Chem.* **1991**, *30*, 815.

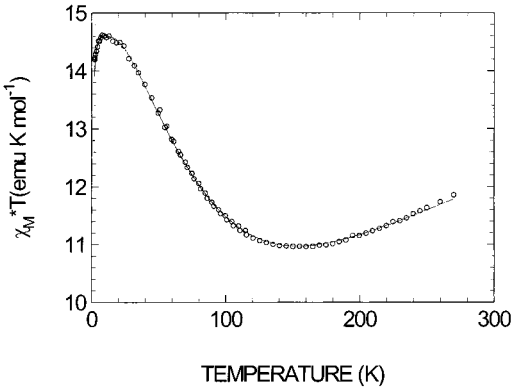

Figure 2. Temperature dependence of the χT product for **1**. The solid line is calculated with $J = 21.1$ cm^{-1}, $J' = -1.1$ cm^{-1}, and $D(S = 5) = -0.2$ cm^{-1} (see text).

bridging methoxide units only supporting the tetranuclear skeleton of the cluster. The same feature was previously observed in quite a few methoxoiron(III) complexes assembled by β-diketonate-assisted methanolysis, namely $[Fe_2(OCH_3)_2(L')_4]$, $[KFe_3(OCH_3)_7(L')_3]$, and $[MFe_6(OCH_3)_{12}(L')_6]^+$ (M = Li, Na; L′ = β-diketonate).[19] The nearest-neighbor Fe···Fe separations in this class of compounds falls in a quite narrow range (3.09−3.24 Å), and the metal ions are invariably arranged in a planar fashion, "sandwiched" by two layers of oxygen atoms.

Static Magnetic Properties. The χT vs T plot for **1** is shown in Figure 2. χT is 11.9 emu K mol^{-1} at 270 K and decreases on lowering the temperature, going through a minimum at $T \approx 155$ K ($\chi T = 10.96$ emu K mol^{-1}), and then increases reaching the value of 14.62 emu K mol^{-1} at 7 K. Below this temperature a small decrease is observed.

The temperature behavior of χT is typical for antiferromagnetic coupling in a system whose spin topology does not allow full compensation of the magnetic moments. In the present case the antiferromagnetic interaction between the central iron ion and the peripheral ones, mediated by the methoxo bridges, leads to a ground state with $S = 5$ and the spin structure schematized below, where all the peripheral spins are aligned parallel to each other but antiparallel to the central one. The observed χT value at the maximum is in good agreement with the value expected for an $S = 5$ with $g = 2$, 15 emu K mol^{-1}. A quantitative

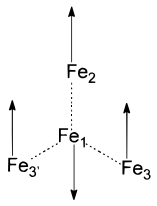

analysis of the magnetic data assuming one exchange coupling constant, using the exchange Hamiltonian $H_{ex} = J(\mathbf{S_1}\cdot\mathbf{S_2} + \mathbf{S_1}\cdot\mathbf{S_3} + \mathbf{S_1}\cdot\mathbf{S_{3'}})$, gives a poor fit of the experimental data ($g = 1.99$ and $J = 22.5$ cm^{-1}), and no significant improvement is achieved by introducing two different J's to take into account the C_2 symmetry of the cluster. A satisfactory fit, shown in Figure 2, is instead obtained if the next-nearest neighbor interactions between peripheral iron ions, described by the Hamiltonian $H'_{ex} = J'(\mathbf{S_2}\cdot\mathbf{S_3} + \mathbf{S_3}\cdot\mathbf{S_{3'}} + \mathbf{S_2}\cdot\mathbf{S_{3'}})$, are taken into account. The best fit parameters are $g = 1.97$, $J = 21.1$ cm^{-1}, and $J' = -1.1$ cm^{-1}. The presence of next-nearest neighbor interactions in clusters of this spin topology has already been taken into account to reproduce the magnetic properties of

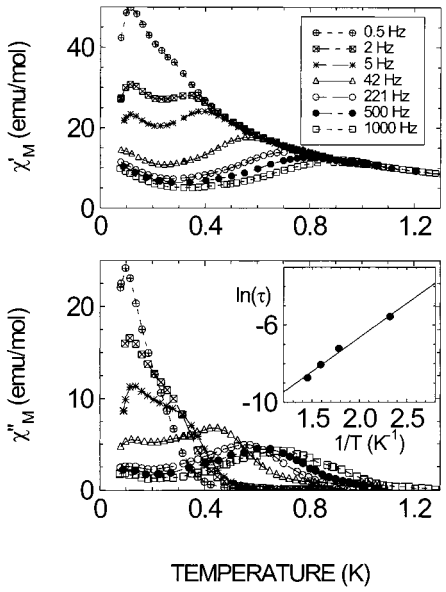

Figure 3. Temperature dependence of the real (top) and imaginary (bottom) components of the ac susceptibility of **1** measured at seven frequencies. The inset shows the temperature dependence of the relaxation time evaluated from the maximum in χ'' (dots). The dashed line corresponds to the Arrhenius behavior that better reproduces the experimental trend.

chromium(III) clusters for which $J'/J \approx 0.1$.[23] The first excited state is a double-degenerate $S = 4$ state lying ca. 60 cm^{-1} above the $S = 5$ ground state. The degeneration arises from the 3-fold symmetry that we have assumed for the cluster. The best fit J value is in the range expected for dialkoxo-bridged iron(III) complexes[20,24] and well agrees with the value $J = 22.1$ cm^{-1} calculated by using an empirical relation between J and the length of the bridge established for iron(III) oxo-bridged dimers.[24a]

The small decrease of χT observed below 7 K is not due to saturation as is observed also in a weak magnetic field (10 mT) and might be originated either by intercluster antiferromagnetic interactions or by the presence of zero field splitting of the ground $S = 5$ spin multiplet. The absence of significant intermolecular contacts as well as the EPR spectra, discussed below, suggest that the latter hypothesis is the most probable.

Dynamic Magnetic Properties. The dynamic magnetic susceptibility of **1** at very low temperature is shown in Figure 3. The real component, χ', increases on lowering temperature, as expected for a paramagnet, down to ca. 1 K. Below this temperature it goes through a maximum, whose position strongly depends on the frequency of the oscillating field. In the same temperature range the imaginary component, χ'', becomes different from zero and shows a frequency-dependent maximum, which is observed at lower temperatures compared to χ'. Below 0.2 K a further increase in χ' is observed, with a sharp maximum at frequencies lower than 100 Hz. While the anomalies observed in the 0.5−1.0 K range agree with the typical behavior of superparamagnets and slow relaxing magnetic molecular clusters,[7,9,25] the very low temperature behavior might be due to long-range ordering of the magnetic moments. In other molecular superparamagnets, as $Mn_{12}Ac$[5,7,25] and Fe_8,[14] such a behavior was

(23) Murray, K. *Adv. Inorg. Chem.* **1995**, *43*, 261.
(24) (a) Gorun, S. M.; Lippard, S. J. *Inorg. Chem.* **1991**, *30*, 1625. (b) Kurtz, D. M. *Chem. Rev.* **1990**, *90*, 585.
(25) Novak, M. A.; Sessoli, R. In *Quantum Tunneling of the Magnetization*; Gunther, L., Barbara, B., Eds.; NATO ASI Series E, Vol. 301; Kluwer: Dordrecht, The Netherlands, 1995.

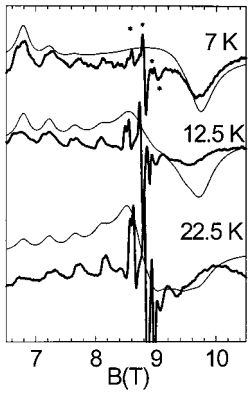

Figure 4. HF-EPR spectra at 245 GHz and three different temperatures of a polycrystalline sample of **1** pressed in a pellet (bold) and simulated spectra assuming $S = 5$ (see text). The bands marked (*) are assigned to the excited multiplets and are not reproduced by the simulation.

not observed because the magnetic moments are essentially frozen at very low temperature, where the weak intercluster dipolar interactions become effective.

The maxima in the out-of-phase component of the susceptibility provide the relaxation time of the magnetization, which is given in an Arrhenius plot in the inset of Figure 3. The few available points agree with a thermally activated behavior, with $\tau_0 = 1.1 \times 10^{-6}$ s and $\Delta = 3.5$ K. The pre-exponential factor compares well with the values observed in other slow relaxing clusters.[5,14,25,26] For these clusters the energy of the barrier has been related to the zero field splitting of the ground spin state.[5,14] To check if this is the case also EPR spectra of **1** were recorded.

EPR Spectra. HF-EPR has been shown to provide important information on the energy levels of the clusters.[27] The spectra recorded at 245 GHz on **1**, shown in Figure 4, have several lines below the resonance of the free electron (8.75 T) and a broad band at higher field. The spacing of the lines at low field is roughly regular and can be attributed to a fine structure arising from the zero field splitting of the ground $S = 5$ multiplet. While at low temperature the most intense line of the regular pattern is the one at lowest field, on increasing the temperature the intensity moves toward the center of the spectrum. A similar trend is observed on the high-field feature even if the fine structure is not resolved. On increasing temperature a set of narrow signals at $g = 2$ also gains intensity, suggesting that it can be attributed to excited spin multiplets. They are marked with an asterisk in Figure 4.

The use of HF-EPR has the advantage of simplifying the spectra because the Zeeman term dominates over the terms related to the zero field splitting, which acts as a second-order perturbation. In the limit of strong field an $S = 5$ spin multiplet with uniaxial magnetic anisotropy should give a spectrum with 10 lines, corresponding to the $-5 \rightarrow -4$, $-4 \rightarrow -3$, $\cdots$, $4 \rightarrow 5$ transitions. In a powder averaged spectrum 10 lines arise from the crystallites with the unique axis parallel to the field, which are separated by $2D/g\mu_B$. The g factor of iron(III), a ^{6}S ion, is close to the free electron value and can be considered as quasi isotropic.[13] The crystallites with the unique axis perpendicular to the magnetic field give also 10 lines with a separation which is half of the previous one, while the contributions of intermediate orientations is averaged to zero in the first-derivative spectrum by the integration over the powder distribution.

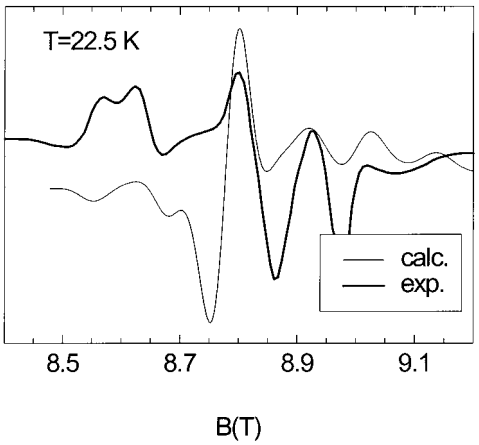

Figure 5. Expanded view of the central structure of the spectrum of **1** at 245 GHz and 22.5 K (bold) and simulated spectrum assuming $S = 4$ (see text).

In the high magnetic field used in these unconventional EPR experiments, the most negative M states of the $S = 5$ multiplet are selectively populated at low temperature, and therefore at low temperature, the lines relative to the transition $-5 \rightarrow -4$ are the most intense and occur at $H = (g_e/g)H_0 + 9D/g\mu_B$ when the field is parallel and at $H = (g_e/g)H_0 - {}^9/_2 D/g\mu_B$ when the field is perpendicular to the unique axis. The fact that the low-field parallel transition is enhanced on decreasing temperature is an unambiguous indication that D is negative. This implies an Ising-type magnetic anisotropy with the unique axis corresponding to the preferential direction of magnetization.

Simulated spectra are also shown in Figure 4. They have been obtained by using a perturbative approach, with $D = -0.20$ cm^{-1}, $g_{\|} = 2.003$, and $g_{\perp} = 2.023$. The number and the positions of the features and their temperature dependencies are correctly reproduced. The features marked with an asterisk were assigned to transitions within excited $S = 4$ multiplets, and they were independently fit. The introduction of a rhombic term in the spin Hamiltonian gives no significant improvement to the simulation.

Attempts were made also to fit the spectra close to the limit of large rhombic anisotropy ($E/D = 0.33$). Although the low-field features were reproduced, the high-field portion of the spectrum could not be satisfactorily reproduced. Further the calculated temperature of the spectra was less satisfactory. We are then inclined to prefer the axial fit. Single-crystal experiments should provide the final answer.

The simulation of the narrow signals centered at $g = 2$ is shown in detail in Figure 5. The best fit parameters assuming $S = 4$, are $D = -0.085$ cm^{-1}, and $E/D = 0.082$. The signal intensity follows the pattern expected for an excited multiplet. The exact simulation of the spectra is made difficult by the partial overlap with the spectra of the ground $S = 5$ multiplet. A confirmation of the assignment could be found also in X-band spectra shown in Figure 6, which do not show the spectra of the ground $S = 5$ state, due to its too large zero field splitting. The variation of the signal intensity of the X-band EPR with temperature is consistent with a multiplet lying ca. 60 cm^{-1} above the ground $S = 5$ state, as found from the fit of the DC magnetic susceptibility measurements. The transitions of the $S = 4$ multiplet in this case are the best resolved at low frequency, and they dramatically decrease their intensities with decreasing temperature below 80 K.

The successful simulation of the spectra using a single spin Hamiltonian suggests that intercluster interactions are very weak

(26) Luis, F.; Bartolomé, J.; Fernández, J. F.; Tejada, J.; Hernández, J. M.; Zhang, X. X.; Ziolo, R. *Phys. Rev. B* **1997**, *55*, 11448.
(27) Barra, A. L.; Brunel, L. C.; Gatteschi, D.; Pardi, L.; Sessoli, R. *Acc. Chem. Res.* **1998**, *31*, 480.

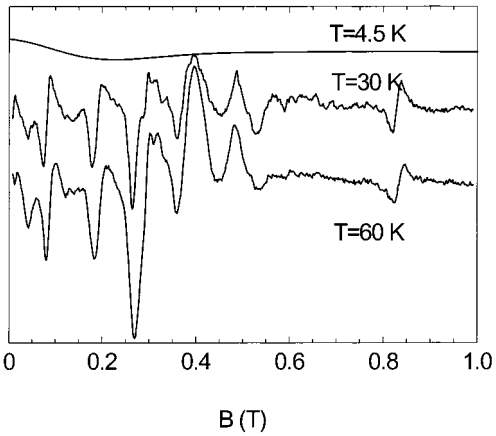

Figure 6. Temperature dependence of the X-band EPR spectra of a polycrystalline powder of **1** pressed in wax.

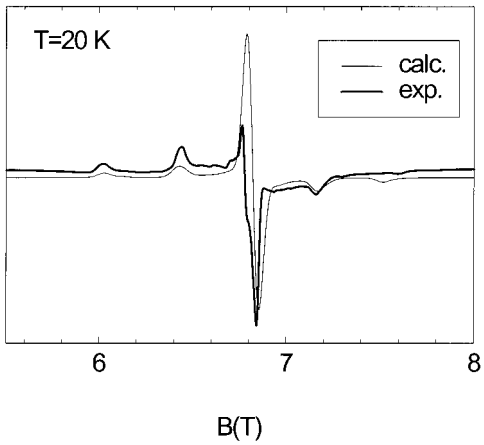

Figure 7. HF-EPR spectrum of a polycrystalline sample of $Fe(dpm)_3$ pressed in a pellet recorded at 190 GHz and 10 K (bold). The standard line corresponds to the simulation (see text).

as expected for the presence of the bulky *tert*-butyl groups on the ligands. The experimentally determined zero field splitting of the ground $S = 5$ spin multiplet can reproduce the small decrease in the χT product at low temperature, as shown in Figure 2, where the solid line is the χT value calculated for a powder average using $S = 5$ and $D = -0.20$ cm^{-1}. Using (2) the height of the barrier is calculated as 7.2 K, which is much larger than that obtained from AC susceptibility measurements. It seems to be general that relaxation measurements provide smaller barrier in single-molecule magnets as compared to that calculated through the ZFS: for $Mn_{12}Ac$, this has been explained with thermally assisted quantum tunneling effects.[25,26] In the present case the experimental uncertainty in the determination of the barrier through relaxation measurements does not allow at the moment to draw any conclusion.

Zero Field Splitting in Iron(III) Complexes. The experimental data reported above provide clear indication of a negative zero field splitting. To understand if this is compatible with single ion contributions, we calculated the zero field splitting tensor of individual iron(III) ions through a ligand field approach, within the AOM formalism. Programs are now available which can calculate the D and E parameters in any coordination environment.[28]

The Hamiltonian $H = H_{AOM} + H_{er} + H_{soc}$ (H_{AOM} is the ligand field Hamiltonian expressed in terms of AOM parameters, H_{er} is the electron repulsion Hamiltonian, and H_{soc} is the spin−orbit coupling one) is calculated using all of the states arising from the d^5 configuration. The Zeeman splitting of the ground state is calculated for each orientation of the magnetic field and compared with the solution of an appropriate spin Hamiltonian. Finally, the parameters of this Hamiltonian are evaluated through a fitting procedure.

We performed first some calculation on model systems, considering trigonal chromophores, with either compression or elongation distortion. The ligand field parameters were fixed at the Dq ($=3e_\sigma - 4e_\pi$) values reported for β-diketonates (1460 cm^{-1}), with $e_\pi/e_\sigma = 0.25$.[29] Trigonal distortions of 5° from octahedral symmetry provide $D = -0.340$ cm^{-1} for elongation and $D = 0.420$ cm^{-1} for compression. This is an interesting result because it shows that even relatively small perturbations on octahedral symmetry can produce sizable zero field splittings in d^5 ^{6}S ions. With these exploratory calculations in hand we looked for real systems on which to test the model; therefore, we tried to fit the zero field splitting tensor of $Fe(acac)_3$ (acac = acetylacetonato) for which EPR data are available.[30] X-band EPR spectra were fit with $|D| = 0.16$ cm^{-1} and $E/D = 0.3$, but no sign for the axial parameter could be obtained. It must be stressed that for a completely rhombic spectrum, characterized by $E/D = {}^1/_3$, the sign of D does not really matter because a change in the sign corresponds to a change in the labels of two axes, say z and x, which in the low symmetry of the environment are arbitrary, except in the presence of single-crystal data. The calculations were performed by assuming identical AOM parameters for all the oxygen atoms and using the atomic coordinates seen in the crystal structure. The parameters of the interelectronic repulsion Hamiltonian for this complex have been fixed at the values reported in the literature: $B = 536$ cm^{-1}, $C = 3260$ cm^{-1}.[31] The ligand field parameter was fixed at $Dq = 1470$ cm^{-1}, while the value of the orbital reduction factor, k, was assumed to be 0.875. The agreement with experiment was excellent: $D = 0.175$ cm^{-1}, $E/D = 0.3$.

To have a further test on the validity of the AOM approach, we recorded the HF-EPR spectra of $Fe(dpm)_3$, given the presence in **1** of the dpm ligand. In the crystal structure of $Fe(dpm)_3$ there are two crystallographically independent molecules in the unit cell. The two molecules have very similar structures: the differences in bond lengths are not larger than 0.02 Å, and the differences between the O−Fe−O angles are always smaller than 1°.[32] The spectra recorded at 190 GHz are shown in Figure 7. A qualitative analysis immediately confirms the $S = {}^5/_2$ ground state, with essentially five sets of features symmetrically centered around $g = 2$. There is some splitting of some of the lines, but it is not possible to clearly distinguish the signal that must be attributed to the two different molecules. Therefore we attempted a simulation assuming a single $S = {}^5/_2$ system. The agreement with the experimental spectra can be considered as satisfactory, as shown by the calculated spectra of Figure 7, obtained with $D = -0.18$ cm^{-1} and $E/D = 0.25$, i.e. with parameters that are pretty close to those of $Fe(acac)_3$. Using for $Fe(dpm)_3$ the same field model used for $Fe(acac)_3$, we evaluated for the two nonequivalent molecules the parameters $D = -0.20$ cm^{-1} with $E/D = 0.29$ and $D = 0.19$ cm^{-1} with $E/D = 0.31$, in reasonable agreement with experimental values considering the complexity of the system and the above considerations on the sign of D. It is interesting to notice that

(28) Bencini, A.; Ciofini, I.; Uytterhoeven, M. G. *Inorg. Chim. Acta* **1998**, *274*, 90.
(29) Bencini, A.; Benelli, C.; Gatteschi, D. *Coord. Chem. Rev.* **1984**, *60*, 131.
(30) Collison, D.; Powell, A. K. *Inorg. Chem.* **1990**, *29* , 4735.
(31) Fatta, A. M.; Lintvedt, R. L. *Inorg. Chem.* **1972**, *11*, 88.
(32) Baidina, I. A.; Stabnikov, P. A.; Alexeev, V. I.; Igumenov, I. K.; Borisov, S. V. *Zh. Strukt. Khim.* **1986**, *27* , 102.

Table 3. Calculated Zero Field Splitting Parameters for the Three Structurally Nonequivalent Iron Sites and for the $S = 5$ Ground State of the Cluster

	Fe2	Fe3	Fe1	single ion $S = 5$	dipolar $S = 5$	total $S = 5$
D_{xx}	−0.0628	0.0022	−0.0292	−0.0147	−0.0229	−0.0375
D_{xy}	−0.0429	0.0190	0.0086	0.0002	0.0016	0.0016
D_{xz}	0	0.0525	0	0	0	0
D_{yy}	0.1455	−0.0655	.0139	0.0045	0.0140	0.0185
D_{yz}	0	0.0786	0	0	0	0
D_{zz}	−0.0827	0.0639	.0154	0.0104	0.0090	0.0194
D	0.231	0.189	−0.046	−0.022	−0.045	−0.056
E/D	0.0247	0.213	0.002	0.027	0.073	0.009
θ^a (deg)	−9.1	67.9	−9.0	1.5	−0.4	0.5

[a] The angle between the principal direction of the tensor and the pseudo-C_3 axis is defined as the perpendicular to the plane comprising the four iron atoms.

in both investigated systems largely rhombic spectra were anticipated by simply using the geometrical coordinates seen in the crystal structure. Since the observation of largely rhombic spectra with $g = 4.3$ is a common feature in iron(III) complexes,[13] both in simple complexes and in biologically relevant compounds, it is rewarding to see how a simple ligand field model can easily reproduce them.

Origin of the Magnetic Anisotropy in 1. Having so obtained some initial guess of the relevant ligand field parameters we proceeded to the calculation of the zero field splitting parameters for the individual iron(III) ions present in **1**. For the calculations we took into consideration the presence of different ligands around the four iron atoms: for dpm we used the *Dq* value reported for $Fe(dpm)_3$[31] ($Dq = 1460$ cm^{-1} for an average bond length of 1.994 Å). No direct information is available about the ligand field strength of methoxy groups bound to Fe(III). Nevertheless it is possible to estimate *Dq* considering that its value is empirically given by the product of two factors, one depending only on the ligand and the second only on the metal.[33] From the reported *Dq* value of methoxy complexes of other metal ions (Co(II), Ni(II), Cr(III))[34] we estimated *Dq* for methoxide ligand bound to iron(III) in the range 1400−1460 cm^{-1}. Our calculations were carried out assuming a value of 1430 cm^{-1} for a bond length of 1.983 Å. The effects associated with the differences in bond lengths were considered assuming a ligand field dependence on $1/r$;[6,35] however, the resulting zfs parameters are not very sensitive to small variation of bond lengths. More important are the low-symmetry effects associated with distortions of the bond angles, which were accounted for by using for the ligands the coordination seen in the crystal structure. Finally, the electron repulsion *B* and *C* parameters for the ion coordinated to CH_3O^- were estimated on the basis of the reported similarity between the ligand fields of methoxide and water.[33] We therefore assumed $B = 950$ cm^{-1} and $C = 2700$ cm^{-1}; we took these values for the central iron, and we averaged them with those of dpm ligand for the peripheral iron atoms ($B = 680$ cm^{-1}, $C = 3040$ cm^{-1}).

The reference axes were chosen in order to agree with the C_2 symmetry of the molecule: *z* is taken parallel to the crystal *b* axis, and *x*, parallel to *c*. This axis is almost coincident with the approximate C_3 axis of the molecule, which is perpendicular to the plane comprising the four iron atoms. The calculated $\mathbf{D}_i$ tensors for the three structurally nonequivalent iron sites and for the $S = 5$ ground state of the cluster are given in Table 3.

The first observation to be made is that the *D* values for the peripheral iron ions are positive, and their principal directions are in agreement with the different site symmetries (C_2 for Fe2, no symmetry for Fe3 and Fe3′). The *D* value for the central ion is negative and roughly parallel to the $x \approx C_3$ axis, as expected due to the relatively symmetric environment. In fact for this ion the coordination polyhedron can be described as a slightly trigonally compressed octahedron ($\alpha = 2.6°$) with one face rotated away from the other by about 22° around the compression axis. The small zero field splitting observed for this ion results from the opposite effects of the two types of distortion from O_h symmetry: calculations carried on considering each distortion alone give in case of compression $D = 0.210$ cm^{-1} and for the rotation $D = -0.231$ cm^{-1}.

A simple rationalization in terms of angular distortion of the values obtained for the **D** tensors of the peripheral irons is not possible due to the low symmetry of the site. Moreover the effects of the different ligand field strength generated by the different ligands are far from being negligible.

The **D** tensors of the *S* spin states of the cluster are expected to be given by[36]

$$\mathbf{D}_{S,S^*} = \sum_i d_i(S_i,S^*,S)\mathbf{D}_i + \sum_{i>j} d_{ij}(S_i,S_j,S^*,S)\mathbf{D}_{ij} \qquad (4)$$

where $\mathbf{D}_i$ is the individual zero field splitting tensor of ion *i*, $\mathbf{D}_{ij}$ is the tensor describing the spin−spin interaction between ion *i* and ion *j*, and $d_i(S_i,S^*,S)$ and $d_{ij}(S_i, S_j,S^*,S)$ are projection coefficients which depend on the individual spins of ions *i* and *j*, on the total spin, and on all the S^* spins needed to specify the coupling scheme. In the present case a natural choice of coupling scheme is given by coupling S_2 to S_3 to give S_{23}, S_{23} to $S_{3'}$ to give $S_{233'}$, and finally $S_{233'}$ to S_1 to give the total spin *S*. In this way the functions can be labeled as $|S_{23},S_{233'},S\rangle$. The coupling coefficients for the cluster can be calculated following standard techniques.[36] For the ground state, which corresponds to the pure $|5,15/2,5\rangle$ state, they are

$$d_1 = 0.1282$$

$$d_2 = d_3 = d_{3'} = 0.1868$$

$$d_{12} = d_{13} = d_{13'} = -0.1816$$

$$d_{23} = d_{23'} = d_{33'} = 0.2335$$

With these coefficients the contribution of the single ion anisotropy to the *D* tensor of the $S = 5$ ground state is calculated as reported in Table 3. It corresponds only to ca. 10% of the actual value, but it is of the same sign. The unique axis is almost parallel to the pseudo-C_3 axis ($\theta = 0.6°$). A negative *D* value for the cluster results from a summation where only the central ion provides a negative contribution. This is the effect of the large cancellation of the $D_{\alpha\beta}$ components in the *yz* plane due to the pseudo C_3 symmetry of the cluster.

The dipolar contribution for $S = 5$ can be calculated using (4) and the point dipole approximation to evaluate the $\mathbf{D}_{ij}$ tensors. The estimated value, given in Table 3, is about 25% of the experimental value and of the same sign.

The sum of dipolar and single ion contribution results in a final value for the $S = 5$ state which is also reported in Table 3. This is about 30% of the experimental value, with negative sign as expected and almost parallel to the pseudo C_3 axis, $\theta = 0.5°$. Even if we have no information on the orientation of the

(33) Lever, A. B. P. *Inorganic Electronic Spectroscopy*; Elsevier: Amsterdam, 1984.
(34) Adams, R. W.; Bishop, E.; Martin, R. L.; Winter, G. *Australian J. Chem.* **1966**, *19*, 207.
(35) Weihe, H.; Güdel, H. U. *J. Am. Chem. Soc.* **1997**, *119*, 6539.
(36) Bencini, A.; Gatteschi, D. *EPR of Exchange Coupled Systems*; Springer-Verlag: Berlin, 1990.

easy axis this last result is quite reasonable if we consider the structure of the molecule. Finally, the *E*/*D* value, 0.078, obtained by this calculation is compatible with the unresolved rhombicity of the powder HF-EPR spectra.

This type of analysis might in principle be extended to the excited multiplets. In the present case we have an experimental estimation of the zero field splitting of the first excited states; however, the presence of quasi-degeneracy of two $S = 4$ states does not allow the use of this simple approach.

Conclusions

In the effort to design molecular clusters exhibiting magnetic bistability due to the presence of large Ising-type magnetic anisotropy, it is of primary importance to be able to rationalize its origin.

We have shown that indeed **1** is another example of slow relaxing magnetic cluster. Its blocking temperature is low, due to the fact that the spin in the ground state is only $S = 5$ and that the ZFS is also small ($D = -0.2$ cm^{-1}). However the anisotropy is of the Ising type, as required in order to observe superparamagnetic-like behavior.

The small size of the cluster allowed a detailed characterization of the zfs and semiquantitative information could be provided by a simple ligand field model. Even if this approach revealed to be more powerful in predicting the zfs of mononuclear symmetric complexes, we have however obtained some precious information. The dipolar contribution to the magnetic anisotropy is far from negligible in iron(III) clusters and in this sense the shape of the cluster can play a significant role in determining its magnetic anisotropy. Large angular distortions from octahedral symmetry not necessarily lead to large zfs as the contributions of different types of distortion can cancel each other.

The difficulties in quantitatively reproducing the value of the parameters may be justified by considering the low symmetry effects and the large amount of approximation necessary in a ligand field approach. In this particular case, the scarcity of spectroscopic data, from which the electronic parameters (Dq, B, C, e_σ/e_π) might be more accurately deduced, limits the validity of the method at a semiquantitative level but better results are expected for clusters comprising different metal ions.[37]

Acknowledgment. We thank A. Bencini for providing the program for AOM calculation and G. L. Abbati for helpful discussion. C.S. thanks C. Paulsen and the CRTBT-CNRS in Grenoble for hospitality and financial support. The financial support of MURST and CNR is gratefully acknowledged.

Supporting Information Available: Text giving X-ray crystallographic data for **1**, a fully labeled ORTEP plot, and a figure showing the crystal packing (PDF). This material is available free of charge via the Internet at http://pubs.acs.org.

JA9818755

(37) Barra, A. L.; Gatteschi, D.; Sessoli, R.; Abbati, G. L.; Cornia, A.; Fabretti, A. C.; Uytterhoeven, M. G. *Angew. Chem., Int. Ed. Engl.* **1997**, *36*, 2329.